Recent North Greenland temperature warming and accumulation

Helle Astrid Kjær[1], Patrick Zens[1], Ross Edwards[3], Martin Olesen[4], Ruth Mottram[4], Gabriel Lewis[5], Christian Terkelsen Holme[1], Samuel Black[1,2], Kasper Holst Lund[1], Mikkel Schmidt[1], Dorthe Dahl-Jensen[1,9], Bo Vinther[1], Anders Svensson[1], Nanna Karlsson[7], Jason E. Box[7], Sepp Kipfstuhl[6], and Paul Vallelonga[1,8]

1Physics for Ice, Climate and Earth Sciences (PICE), Niels Bohr Institute, University of Copenhagen, Copenhagen 2100, Denmark
2 NatureScot, Inverness, IV3 8NW, United Kingdom
3Physics and Astronomy, Curtin University, Perth, Western Australia, Australia
4Danish Meteorological Institute, Copenhagen 2100, Denmark
5Department of Earth Sciences, Dartmouth College, Hanover, NH, USA
6Alfred-Wegener-Institut Helmholtz-Zentrum für Polar- und Meeresforschung, Bremerhaven, Germany
7Geologic Survey of Denmark and Greenland (GEUS), Copenhagen 1350, Denmark
8UWA Oceans Institute, University of Western Australia, Crawley, WA, Australia
9University of Manitoba, Winnipeg, MB R3T 2N2, Canada

Correspondence to: Helle Astrid Kjær (hellek@fys.ku.dk)

Abstract. In a warming climate concise knowledge of the mass balance of the Greenland ice sheet is of utter importance. Speculations that current warming will increase the snow accumulation and mitigate mass balance losses are unconstrained as accumulation data across large regions of the northern ice sheet are scarce. We reconstructed the accumulation from six north Greenland shallow firn cores (~10m) and eight snow cores (~2m) to constrain recent accumulation patterns in northern Greenland and calculated recent warming in the same area using borehole temperature measurements.

We find an increase in temperatures in the north Greenland interior of 0.9 to 2.5 °C (method and site dependent) per decade over the past two decades in line with an Arctic amplified anthropogenic warming. We compare annual reconstructed accumulation from the firn cores (1966-2015) to radar estimates and to annual re-analysis data (1980-2016) of precipitation subtracted evaporation from the regional climate model HIRHAM5, operated by the Danish Meteorological Institute. The spatial variability resembles that observed in earlier estimates with a clear increase west of the topographic divide and a low accumulation area across the north-eastern ice sheet. Our accumulation results are comparable to earlier firn core estimates, despite being larger in the east. We only find a positive significant trend in the accumulation for the period 2000-2010 to the northwest.

In the vicinity of the EGRIP deep ice core drilling site, we find variable accumulation patterns for two 15 km apart firn cores likely owing to local topographic effects as a result of the North East Greenland Ice Stream dynamics.

1 Introduction

The Arctic today is warming and automated weather stations from the Greenland Climate Network (GC-net) (Steffen and Box, 2018) and at Summit Station in central Greenland McGrath et al. (2013) have identified Greenland warming trends even in the central part of the ice sheet of 0.9 °C/decade. From the Clausius-Clapeyron relationship one would expect an accumulation change following increasing temperatures, as was demonstrated by Box (2013) who found an increase of 6.8% K^{-1}.

Greenland's contribution to sea-level rise is currently estimated at ~10 cm by 2100 (Lewis et al., 2017; Muntjewerf et al., 2020). The uncertainty of this number is in part due to the surface mass balance (SMB, i.e. precipitation minus evaporation, sublimation, meltwater runoff and/or erosion). Precise knowledge of the accumulation is crucial to constrain the ice sheet SMB. For the ice sheet interior the most precise data of accumulation are from ice cores, however, they are sparse and most do not cover the recent period 2010-present (Box et al., 2009; Montgomery et al., 2018), or the northern region of the ice sheet (Koenig et al., 2016; Montgomery et al., 2018). Satellite radar altimetry data sets over the Greenland ice sheet (GrIS) begin as

late as 1991. These data provide invaluable information on accumulation and temperature used for monitoring the current changes of the ice sheets due to the dense spatial and temporal coverage they offer (Koenig et al., 2016; Sandberg Sørensen et al., 2018; Simonsen and Sørensen, 2017). However uncertainties are large as only limited ground truth data is available in the form of snow and firn cores covering the satellite era (Bales et al., 2009; Box, 2013). Given the large area it can cover, ground

5   penetrating radar (GPR) offers a potential solution. However, it also relies on a reference point, normally in the form of an accumulation layer of known depth and age, meaning that GPR data is seldom available in annual resolution. As one of the few methods available for constraining both satellite and GPR data, the collection of firn cores is therefore crucial.

With regard to the Greenland ice sheet's accumulation, studies including central Greenland are in disagreement, with results ranging from strongly decreasing to slightly increasing accumulation in recent times dependent on the exact region (Lewis et

10   al., 2017). Mosley-Thompson et al. (2001) studied the period up to 1998 and mainly south of 72°N and showed that accumulation has indeed changed. They also found evidence for decadal timescale variability, speculated to be caused by the North Atlantic Oscillation (NAO) as opposite trends in northwest and central Greenland were observed. Burgess et al. (2010) expanded upon the study with additional ground truth data and found an interannual variability of 18% and an increase in accumulation of 7 mm w.eq. per decade. Miège et al. (2013) found no significant temporal trend in south-east Greenland using

15   three 50 m firn cores and radar. Hawley et al. (2014) used snow and firn cores and ground penetrating radar to investigate the trend in accumulation in northwest and central Greenland and, when compared to older snow pits in the area, found positive trends of 2.2–3.1 cm w.eq., equivalent a 10% change in the dry snow region over 52 yrs. Using a combination of modelling (RACMO2) and firn cores, Box (2013) found an accelerated increase in accumulation in most of Greenland between 1840 and 1996 compared to the period 1600 onwards, with the exception of localised decreases (5%) in the north-east. Buchardt et al.,

20   2012 compared ice core accumulation with water isotopes (a proxy for temperature) and found no conclusive trends for accumulation, but did demonstrate an increase in $\delta^{18}O$ for the most recent decade, speculated to correspond with increasing temperature. Using a combination of radar, shallow cores and climate modelling, Lewis et al., 2017 observed a decrease in the accumulation rates in the western Greenland accumulation zone of 9 mm.w.eq. per year, while further analysis by Lewis et al. (2019) revealed decreasing accumulation of 2.5% annually for the period 1996-2016. Recently, the Surface Mass Balance and

25   snow on Sea Ice working group presented a compilation of accumulation data in Greenland, known as the SUMup dataset. (Montgomery et al., 2018). The SUMup compiled accumulation dataset includes many of the above mentioned datasets and covers 36 sites in Greenland. However, only 10% of the snow and firn cores in the dataset were retrieved after 1999 (excluding Summit station data) and just 5% of them are from north of 76N. Thus, there is a need for enhanced ground truth measurements to constrain the effect of recent temperature changes on accumulation, especially in northern Greenland.

30

Ice, firn and snow cores from the Greenland ice sheet offer a unique opportunity to constrain the recent trend in Greenland accumulation. Ice cores analysed in sufficient resolution e.g. by means of continuous flow analysis (CFA, (Bigler et al., 2011)) provide information about ancient atmospheric aerosol concentrations, most of which have annual peaks. These cyclic peaks can be used to constrain annual layers and, if the density is known, to reconstruct historic snow accumulation rates (Gfeller et

35   al., 2014).

The principle of CFA includes the continuous melting of ice cores and the immediate analysis of separate chemical proxies by individual detection units. This happens within a sealed system, which ensures the lowest possible risk of contamination and sample loss (Röthlisberger et al., 2000). Such high resolution data allow for identification of annual layers and even sub annual events (Svensson et al., 2008; Winstrup et al., 2012). Water isotopes, a proxy for temperature, is commonly used for such

40   annual layer identification, however in low accumulation areas diffusion can smooth the water isotope signal to an extent that annual layers are no longer reliable. In such areas one can use other proxies with annual cycles. For example, in shallow firn cores hydrogen peroxide, which is naturally produced in the atmosphere by photochemical derived self-reaction of hydroperoxyl radicals (HO_2), can be used to identify seasonality as the production of H_2O_2 mainly takes place during months

of intense insolation. Therefore, firn core records show maximum concentrations in the summer and minimum concentrations during the winter months when photochemical processes are absent at polar latitudes. This strong seasonal pattern creates an excellent proxy that is commonly used for dating polar ice cores (Sigg and Neftel, 1988) and thus can be used to reconstruct accumulation (Frey et al., 2006).

In this study accumulation have been reconstructed at 14 sites in northern Greenland. To do so, six shallow firn cores down to 14 m were collected during a traverse (N2E) in 2015 from the deep ice core site NEEM (77°25.219',51°09.588' W) to the deep ice core site EastGRIP (75°37.501' N, 23°58.809' W), alongside eight snow cores in 2017 down to 2 m traversing from Kangerlussuaq in the west to the EastGRIP site. Snow and firn cores were analysed at the Niels Bohr Institute in Copenhagen

10   for chemical impurities. The impurities, especially the H_2O_2, were used to constrain annual layers. Densities in 55 cm resolution were also collected in the field for the 6 shallow cores. With the 6 new cores and snow cores we thus constrain the northern Greenland accumulation over the recent decades (up until 2016) and provide much needed ground truth information.

Additionally, to evaluate the sites temperature trend in the recent decades, we obtained the 10 m depth borehole temperature in each location, taken to represent the annual mean temperature, and compared it to previous measurements from NGT

15   traverse in 1993-1995 (Fischer et al., 1998; Weissbach et al., 2016).

Both reconstructed accumulation and temperatures are compared to results from the Danish Meteorological Institute regional climate model HIRHAM5, forced at the lateral boundaries by re-analysis data (DMI, (Christensen et al., 2006)). The reconstructed accumulation is further compared to earlier available estimates from firn and ice cores (Montgomery et al., 2018; Schaller et al., 2016), recent radar estimates (Karlsson et al., 2020; Lewis et al., 2017) and precipitation-evaporation (P-E) re-

20   analysis data from the HIRHAM 5 model.

2 Methods

2.1. Firn core drilling during the N2E traverse in 2015

The six firn cores were extracted using the American IDDO (U.S. Ice Drilling and Design Operations) hand auger (76 mm diameter) from the surface to a depth between 9.1 m and 14.0 m (Table 1).

25   In the field the cores were split into 0.55 m long segments, – placed in a so-called "Danish bag" and weighed. The cores were then stored in cooler boxes and transported on sledges to the EastGRIP site, flown to Kangerlussuaq and then shipped further to Copenhagen, Denmark for analysis.

The weight of each bag (2 g precision) and the length of each bag (0.5 cm precision) was noted. Thus the density of each 55 m section can be determined with a precision <4% assuming the cores are close to circular with a diameter of 75-76 mm. See

30   supplementary Figure S1.

With the cores extracted, the borehole temperature at 10 m depth was determined by a single thermistor connected to a multimeter using the 4-wire method (+-0.1 °C) (Clow, 1992; Gundestrup et al., 1994; Orsi et al., 2012). The temperature at 10 m depth is a good approximation of the *in situ* mean annual surface temperature in the absence of melting (Dahl-Jensen et al., 1998). Table 2 provides the temperature at 10 m depth for each site representing the annual mean temperature and one

35   can calculate the annual cycle of temperature at such depths is dampened to 5% that observed at the surface (Johnsen et al., 1992).

2.2 Snow tube collection during the 2017 Inuit Windsled Project traverse windsled ice river

During the 2017 Inuit Windsled Project traverse Greenland expedition from Kangerlussuaq to the EastGRIP deep ice core drilling site the upper two m of the snow pack was sampled at eight sites along the route (Table 5, Figure 1). The snow pack

40   was sampled using the "liner technique" as described in Schaller et al. (2016), where 1 m-long hollow carbon tubes are pushed

downward into the snow before excavation and retrieval. The snow from 1-2 m depth was sampled in a similar matter however only for sites north of 73ºN. The cores remained in the carbon tubes after sampling and were stored in cooler boxes carried by the wind driven sledge during transport to EGRIP. From EGRIP the samples followed same path as those collected in 2015.

2.3 Continuous flow analysis

5 Annual layers in the snow and firn cores were identified using the annual peak concentration of impurities, mainly H_2O_2. The Copenhagen CFA system was used to analyse the impurity content in the snow and firn cores. For the 6 firn cores and 8 snow tubes the melt water conductivity, insoluble dust, H_2O_2, NH_4^+, Ca^{2+} and acid were determined (Bigler et al., 2011; Kjær et al., 2016; Simonsen et al., 2018). Firn cores were cut into 3.6 x 3.6 cm squares prior to melting, whereas the snow cores were melted on a full size melt head. In the CFA system the inner section of the core is separated from the outer during continuous

10 melting after which the inner decontaminated line is split into several lines. For each line an ion is determined after the addition of specific reagent and in some cases a buffer by means of fluorescence (NH_4^+, H_2O_2, Ca^{2+}). The soluble dust is measured by a laser instrument (ABAKUS LDS, Klotz, see also Simonsen et al., 2018) and the conductivity of the water is determined using an Amber Science 3082 conductivity metre as presented by Bigler et al. (2011). In addition to the system presented in Bigler et al. (2011) acid was also analysed (Kjær et al., 2016). For every 4-5 metre of firn core, baselines of ultrapure milliQ

15 water were determined and a set of standards were run to calibrate the measurements. Due to the density in the top 2.2 m of each core calibration was carried out at 55 cm melting intervals. The melt speed was kept at 4 cm min^{-1} and with a maximum response time of 30s within the system, the final depth resolution of the ions measured are on the order of 2 cm (acidity, NH_4^+, H_2O_2, Ca^{2+}), while for conductivity and dust a shorter response time for a depth resolution of 8 mm is achieved. The firn pore capillaries caused melt water to be pulled from the melt head into the firn creating some dispersion especially in the low density

20 part of the dataset. The capillary effect was limited by placing a round circular coin between the melt head and the firn, minimizing suction of air into the CFA system and percolation of melt water up into the firn. Even with percolation, the annual peaks in all proxies were well resolved.

2.4 Discrete water isotopes

For the firn cores 2015T-A1 (NEEM site) and 2015T-A5 (EastGRIP site) each bag was also subsampled in 2.5 cm discrete

25 depth sections. Each sample was melted in separate air-tight metal containers and transferred to small vials for the purposes of stable water isotope analysis ($\delta^{18}O$, δD). The measurements were performed using a commercial Cavity Ring-Down Spectroscopy (Picarro L2130) coupled to a high throughput-A0212 vaporiser (Gkinis et al., 2011). The analysis was conducted with a water concentration level in the range 18,000-23,000 ppm in order to minimize the measurement-induced humidity influence on the water isotopic composition. All samples are calibrated with respect to Vienna Standard Mean Ocean Water

30 (VSMOW) and normalized to the VSMOW-SLAP (Standard Light Antarctic Precipitation) scale. The presented measurements all have a precision better than 0.10 ‰ ($\delta^{18}O$) and 0.50‰ (δD), respectively.

The deuterium excess data (d_xs) were corrected for water-isotope specific diffusion which alters the d_xs signal unevenly in the upper firn column. This was achieved by separately back-diffusing the $\delta^{18}O$ and δD records similar to the method outlined in Steen-Larsen et al. (2011). This study uses the diffusivity parameterization of Johnsen et al. (2000) where the magnitude of

35 diffusion depends on isotopic species, surface temperature, density, accumulation rate and pressure at the drill site.

2.5 Core chronology and annual layer counting Techniques

A timescale for each firn and snow core was reconstructed by means of annual layer counting (Svensson et al., 2008; Winstrup et al., 2012). Annual cycles can be identified in the peroxide signal, which peaks in summer due to the photolytic reaction

40 caused by sunlight; the ammonium signal, which peaks in late summer due to biogenic activity; the sodium signal, which peaks

with winter storms; the dust signal, which peaks in spring; and the acid signal, which peaks a little later in spring due to anthropogenic activity and subsequent arctic haze (Gfeller et al., 2014; Kaufmann et al., 2008). In this study we predominantly relied on the seasonality of peroxide (Sigg and Neftel, 1988) and only used the seasonality in other compounds (mainly dust) in the cases where peroxide signals were poorly defined, such as the deeper part of the cores from low accumulation sites;

5   2015T-A6, 2015T-A4 and 2015T-A5. The total age of each core and the uncertainty was defined as +/- 0.5 year for each uncertain year and can be found in Table 1. A5 (EastGRIP site) reaches furthest back in time to 1966, while the youngest core (A1-NEEM site) spans only the period 1998 to 2015.

For the Windsled snow cores collected in summer 2017 we constrained the first peroxide peak to summer 2016 and the second to 2015. In all snow cores the 2016 peak was within the first metre of snow. However, for the most southern cores (<73N)

10   both the 2016 and 2015 peaks were not collected. The uncertainty associated with assigning the summer peak depths in each snow core account to between 5 and 1 cm mainly due to increased dispersion when melting snow as explained above. The largest uncertainties in the year to year accumulation estimates from snow cores exists at the high accumulation sites as a result of the H_2O_2 summer peak being relatively wide. For the snow cores retrieved at 74°09'N and 74°20'N the depth from the surface (spring 2017) to the summer peak of 2016 is less than expected and only on the order of 8-10 cm of snow. This we

15   suggest is caused by low accumulation at the site or sample loss during collection. Thus, as the layer representing summer 2015 to summer 2016 is found in all cores north of 73°N collected with the windsled, it was used as the common reference point from which further analysis and site to site comparisons were made.

2.6 Reconstruction of accumulation

Density measurements were performed in the field for the N2E shallow firn cores on every 55 cm section, as described earlier.

20   The densification profile (supplementary Figure S1) was similar for all 6 sites and we use a linear interpolation to calculate densification rates for each of the six cores.

The annual water equivalent accumulation (A_{yr}) was reconstructed using $A = z * \rho_{sample} / \rho_{water}$, where A is the accumulation in m water equivalent per year (m. w.eq. a^{-1}), z is the thickness of the annual layers in m and ρ_{sample} is their corresponding firn density in kg m^{-3}. The uncertainty associated with the firn density is on the order of 4% and the uncertainty on the peak summer

25   position of the annual layer is on the order of ±1 cm for the N2E firn cores. The combined uncertainty on the annual accumulation amount to less than ±1.1 cm w.eq.

As the windsled snow cores collected in 2017 were not weighed a model density profile was used to reconstruct accumulation. In combination with the depths of the 2016 and 2015 summer peak of peroxide, a fixed density in the top 1 metre of 350 kg m^{-3} was used to reconstruct the accumulation form the snow cores. This value was chosen as Schaller et al. (2016) found

30   densities between 300 and 400 kg m^{-3} in the top 1 m of snow by means of x-ray tomography performed on snow liners from the 2015 N2E traverse.

2.7 Atmospheric modelling

The snowfall accumulation data obtained from the firn cores are compared with that simulated by the Danish Meteorological Institute HIRHAM5 regional climate model for a domain covering Greenland. HIRHAM5 is described in Christensen et al.

35   (2006) and combines dynamics from the numerical weather prediction model HIRLAM7 (Eerola, K, 2006) and physics from the global climate model ECHAM5 (Roeckner et al., 2003). The subsurface scheme in HIRHAM5 has been extended with an off line component that handles liquid water flow and retention on the Greenland ice sheet (Langen et al., 2017). On the lateral boundaries and over open ocean HIRHAM5 is forced with the European re-analysis dataset ERA-Interim from ECMWF (Dee et al., 2011). The HIRHAM5 experiment used in this study has a horizontal resolution at 0.05×0.05 degree (approximately

40   5.5 km) and covers 35 years (1980-2014).

2.8 Ice Bridge radar data

NASA Operation IceBridge radar data were collected during the 2013-2014 summer campaigns and is validated with ten deep ice cores from across the GrIS (Lewis et al., 2017). Accumulation rates were calculated for 18 epochs over 1712 – 2014 to analyse SMB changes and correlations with both the Atlantic Multidecadal Oscillation and North Atlantic Oscillation. The accumulation radar operates in the 600 – 900 MHz range, yielding an uncertainty of 12.7 cm w.eq. a^{-1} for any single epoch, when taking into account the uncertainty on density and annual layer dated isochrones used for a calibration (see Lewis et al., 2017). Here, we choose to compare *in situ* firn core accumulation rates with the closest radar returns from IceBridge flight lines to validate our measurements in tandem with the HIRHAM5 output.

3 Results

3.1 North Greenland temperatures

The temperature at ~10 m depth for each of the shallow core sites (Table 2) are the highest in the north-east (NEEM site –A1 -27.40 °C, A2 -26.74 °C) and ~2 °C lower at the central divide (A3 -29.75 °C) and east of it (EastGRIP site-A5 -29.23 °C). For the cores A1 (NEEM) and A5 (EastGRIP) water isotopes were determined and are shown in supplementary material Figure S3. Annual layers in the water isotopes can be clearly identified in A1, while for A5 the annual signal is lost below 5 m depth corresponding to year 1992. The A1 (A5) core's mean $\delta^{18}O$ and δD values are respectively -32.17 ‰ (-36.16 ‰) and -247.2 ‰ (-281.6 ‰). Using the relationship between mean annual values of $\delta^{18}O$ and temperature on the Greenland ice sheet (Temperature=($\delta^{18}O$+13.7)/0.67 (Johnsen et al., 1992)) the observed mean $\delta^{18}O$ concentrations in the two cores corresponds to -27.6 °C at the northern NEEM site and -33.5 °C east of the divide at EastGRIP and thus suggest much colder temperatures at the EastGRIP sites than those measured in the borehole, while at NEEM the two estimates are in correspondence. However, we recall that water isotopes are not only a function of temperature, but also of accumulation, especially so in North-East Greenland (Buchardt et al., 2012).

Orsi et al. (2017) used borehole temperature from the NEEM main core borehole and observed a mean temperature in the period 1900-1970 of -28.6 °C and thus our estimates of -27.4 °C (borehole) and -27.6 °C (water isotopes) are within uncertainties.

The HIRHAM5 mean temperature in the period 1980-2014 is higher by 0.9 °C to 2.9 °C (Table 2) at the sites compared with the observed 10 m borehole temperatures. However, recall that the borehole temperature is the seasonal cycle damped with time, thus influenced to some extent also by temperature of previous years and that the modelled temperature represents 2 m heights not skin temperatures.

We observe that mainly the winter temperatures from HIRHAM5 are biased compared to observations from weather stations and according to several model specifications can contribute to the winter warm temperature bias. First of all, the vertical resolution of the model is insufficient to resolve the processes that leads to strong temperature inversion. Secondly, the temperature bias can be related to errors in the model parametrization of clouds and in that way related to a biased incoming longwave radiation. And finally, the turbulent exchange near the surface is poorly resolved in HIRHAM5.

In conclusion we find higher temperatures in north-west Greenland than in north-east in both observations and model and note that the HIRHAM5 model is generally warm biased.

3.2 Accumulation from firn and snow cores

The accumulation reconstructed from the 6 firn cores with time is shown in Figure 2 (coloured dotted lines) together with a five year running average trend (coloured full line). In Table 3 decadal accumulation means are presented, while the full core means are presented in the map Figure 1 and Figure 3.

A clear east-west gradient is evident in the reconstructed accumulation (Figure 3) with the highest accumulation found at the NEEM ice core site, 22.2 cm w.eq. yr^{-1} (core 2015 T-A1) and lowest accumulation, 11.8 cm w.eq yr^{-1}, at the ice divide site (core 2015 T-A6). East of the ice divide the accumulation again increases but only slight (13.7 cm w.eq. yr^{-1} –A5). The year to year variability (1 sigma) is 25% of the accumulation at the NEEM site (A1) and decreases towards the ice divide 16% (T-A3), 18% (A6) and increase again at the EastGRIP site (21%-A4, 30 %-A5).

During the traverse also several snow core liners representing just the top 2 m of snow were also collected. The results from these are presented in Schaller et al. (2016) and the snow liners represent accumulation from 2 to 3 years. The comparable sites to the traverse cores from A1 to A6 are N2E02 (A1), N2E06 (A2), N2E09 (A3), N2E19 (A4), N2E22 (A5) and N2E12 (A6) with accumulation of 22.45, 19.35, 15.59, 13.22, 13.96 and 12.47 cm w.eq. yr^{-1} respectively shown also in Figure 2 (grey line). Thus the results from both snow liners and firn cores agree within uncertainties.

The results from the snow cores collected during the windsled traverse in 2017 are shown in Table 5. Note that the accumulation presented from the 2017 snow cores represents just one year (summer 2015 to summer 2016) and a significant variability to the annual mean at the particular sites could be present. The accumulation vary from 24.5 cm w.eq. yr^{-1} at the central ice divide in the south (73.65N, 40.56 W) and decreases to 14.0 cm w. eq. yr^{-1} in the drier region near EastGRIP (75.40N, 27.03W) and we observe a clear decreasing trend from central-south to the north-east in line with other estimates from the region. The site closest to EastGRIP (14.0 cm w.eq. yr^{-1}) is well in line also with the shallow firn core results of 13.7 cm and 14.6 cm w.eq. yr^{-1} for the sites A5 and A4 respectively, though the longer firn cores are further north.

3.3 Accumulation from HIRHAM5 and comparison to firn cores

In general, the HIRHAM5 annual precipitation minus the surface water flux (mainly sublimation) slightly underestimates the net accumulation observed in the firn cores (Figure 3). Furthermore, a linear relationship between the annual accumulation in the firn core and in the model show that the model accumulation is just 66% (R^2 0.74) of the annual mean firn core accumulation (Figure 5), though with better representation at the higher accumulation sites in the west (A1~ 106%). East of the divide HIRHAM5 again estimates a lower accumulation (56-67%) than that observed in the firn cores, suggesting that model performance decreases in the east. For the site A6, HIRHAM5 captures just 55%. However, we also note that the site A6 is very close to where the central ice divide splits into a north-eastern and north-western branch (supplementary Figure S2). Here we speculate that the difference also relates to changes between these topographic features in the model domain and in the real world, as well as the ice divides influence on the dominant precipitation patterns. Further we note that a climate variable from a grid cell in HIRHAM5 represents the mean conditions over an area of 5.5 x 5.5 km and that comparing a variable from a grid point with a point measurement from a shallow ice core should be done cautiously. Pointwise measurements are sensitive to immediate changes in the surrounding area and are thus not necessarily directly comparable to solid accumulation or other weather conditions simulated by HIRHAM5 on a grid of 5.5 km (Lucas-Picher et al., 2012). The annual variability in HIRHAM5 follows the accumulation trend linearly and is between 14 and 18% of the mean accumulation, whilst the annual variability in the firn cores is between 15 and 30% of the accumulation signal and not linearly related to the mean accumulation. This suggests that the firn reconstructions are subject to depositional noise.

The site A4 is at the margin of the ice stream NEGIS. At the ice shear margin zone of the ice stream (Figure 6) there are topographical changes over short distances of up to 40 m (Bamber et al., 2018; Joughin et al., 2010; Vallelonga et al., 2014). The model does not incorporate such detailed topographical features, producing a flat surface at NEGIS in the model domain At site A4 HIRHAM5 underestimates the observed accumulation (63% captured). Topographic undulations cause more of the precipitation to accumulate in the depressions (Miège et al., 2013). Therefore, this difference may be explained by A4's location in a valley on the ice shear margin. Traverse core A5 (just outside the ice stream) is subject also to some of this effect (67% captured) though not to the same extent as A4.

To estimate the area of accumulation that each firn core theoretically represents we compared the accumulated precipitation minus evaporation observed in the model for each site with that in all other model points (Figure 4). In Table 3 annual accumulation correlations between sites in both model and firn cores are shown for the period 1998-2015. It is evident that the

5 three cores west of the divide (A1, A2 and A3) represent large areas and should be well correlated (Figure 4). This is also true in both the model, where correlations (R^2 -Table 4) between A1 and A2 are 0.90 ($p<10^{-6}$) and A2 and A3 are 0.95 ($p<10^{-9}$), and in the firn cores (A1, A2 $R^2=0.56$, $p<10^{-4}$, and A2, A3 $R^2=0.54$, $p<10^{-5}$), despite the influence of depositional noise not represented in the model. The site A6 close to the central divide is also well correlated with A1, A2 and A3 in the reconstructed accumulation from the firn cores, whilst in the model is correlates more strongly with eastern sites.

10 Correlations east of the divide are lower both in HIRHAM5 and in firn cores (Figure 4, Table 3). This may be due to the lower accumulation rates in the east, which decreases temporal resolution in the core and increases uncertainty within and between reconstructed accumulation rates. In addition, precipitation across the north-eastern ice sheet is mostly cyclone related, whereas the western part is predominantly connected to the large scale circulations (Hutterli et al., 2005).

Core T2015-A4 and T2015-A5, which are only 15 km apart, show in the model a very high correlation (0.97, $p\sim10^{-11}$), yet in

15 the reconstructions from the firn cores they only correlate by 0.28. We speculate that the local topography caused by the north East Greenland Ice Stream, which is not fully resolved in the model domain, is causing more variability in the accumulation reconstructed from the firn cores as a result of snow drift and depositional noise induced by such topographic hills (Vallelonga et al., 2014).

4. Discussion

20 **4.1 Increasing temperatures in northern Greenland since the early 1990's**

In 1993-1995 several firn cores were drilled in northern Greenland as part of the North Greenland traverse (NGT (Fischer et al., 1998; Weissbach et al., 2016)). These can be used to evaluate if there has been a trend in the temperature with time by comparing the closest NGT site with our N2E firn core borehole temperatures representing 2014 (Table 2). Our borehole temperatures representing the year 2014 are 2.9 °C (NEEM site, A1), 3.9 °C (A2) and 3.1 °C (A5-EastGRIP) higher than those

25 from the NGT traverse representing 1993/1995. Even when taking the uncertainty of ±0.5 °C into account, this result documents a significant warming. However it should be noted that whilst the borehole 10 m temperature represents annual mean temperature over a period of time, annual temperature variations can distort observed values. Further, the two measurements from the NGT and N2E are not from the exact same site.

30 We found the HIRHAM5 model to be warm biased (1.9 °C [0.86, 2.91]) compared to the borehole temperatures, however its trend with time is in line with the lower estimates of the warming trend observed from the boreholes temperatures. The warming trend for the period 1980-2014 observed in the HIRHAM5 model is for the A1 to A6 sites 0.78, 0.76, 0.79, 0.83, 0.84 and 0.82 °C/decade respectively, with a lower trend if only the period 1993-2014 is used of approximately 0.51 (A1) to 0.68 (A5) °C/decade.

35

The $\delta^{18}O$ and δD data are often used as proxies for temperature, but for the firn cores A1 and A5 a linear increase is not manifested in the isotopic signals with time (Supplementary material Figure S3). Contrary, the difusion corrected (Steen-Larsen et al., 2011) deuterium excess (d_xs=δD – 8* $\delta^{18}O$, Dansgaard (1964)) of the A5 core shows a significant linearly decreasing trend (-0.44 ‰/year) in the period 2000-2015 (Figure 7), where a similar trend in the nearby NEGIS firn core is

40 observed (Vallelonga et al., 2014). Variations in ice core deuterium excess are typically interpreted as reflecting changes at the moisture source region through kinetic effects related to the relative humidity, wind speed and sea surface temperature

(Johnsen et al., 1989; Masson-Delmotte et al., 2005). Here we speculate that the decreasing trend is climatic and related to the moisture source region or unknown (and strong) post-depositional processes that cause the deposited snow's water isotopic composition to kinetically fractionate. The latter seems less likely as this effect would have had to linearly increase its influence on the d_xs signal over the past 15 years. While it is an interesting research question to quantify the cause behind this signal,

5   it remains outside the scope of this paper as it would require studies with isotope-enabled atmosphere general circulation modeling and/or vapor-ice water isotope fractionation experiments at the drill site. We also note that recent papers (Kopec et al., 2019; Madsen et al., 2019) have questioned the use of deuterium excess as a moisture source proxy.

In conclusion our results from both *in situ* snow temperatures at 10 m depth and from the HIRHAM model point to a northern

10   Greenland warming trend over the past 2 decades of between 1.6 and 4.9 °C (Table 2). However, the signature of such an increase is not observed in the $\delta^{18}O$ and δD (Supplementary material Figure S3). Furthermore, the deuterium excess results (Figure 7) point to a strong change for the EastGRIP site (A5), perhaps as a result of local moisture change yet not observed at NEEM (A1). In comparison, Box et al. (2009) found an increasing annual temperature in 1994-2007 of ~1 °C in the interior Greenland ice sheet using a mix of observations. The trend was found to be stronger in winter and spring and less pronounced

15   in summer and in coastal Greenland. An even stronger trend was observed at Station Nord 1.73 °C, Danmarkshavn 0.85 °C and Daneborg 1.27 °C for the period 1991-2000. Hanna et al., (2020) updated the re-analysis to 2019 and observed the same annual variability in trends. Most notably they observed the strongest warming in west and northwest coastal Greenland (total 6–6.5°C in winter for the period 1991-2019), however they also note a flattening of the temperature increase after 2010. The warming we observe is in line with these previous observations. It is worth also noticing that according to our results of the

20   past two decades the warming trend of northern Greenland has already surpassed the temperature trend anticipated for central Greenland from an RCP 8.5 scenario (NorESM model (Jansen et al., 2020)).

4.3 Annual mean accumulation across the northern Greenland ice sheet

We now compare the mean accumulation observed from both of the firn cores 2015 and the snow cores 2017 to those from other reconstructions (Figures 1 and 2). Figure 1 shows the annual mean accumulation reconstruction from Burgess et al.

25   (2010) with the results from this study illustrated as circles. Results from several older firn and snow core studies are also shown and include the 2015 traverse snow core results from Schaller et al. (2016) in triangles facing up, the NGT firn core traverse results from cores taken obtained 1993-1995 shown as tringles facing down (Weissbach et al., 2016) and further snow and firn cores from the compilations of Burkhart et al. (2009) and Montgomery et al. (2018) e.g. many of the PARCA cores taken in the late 90's (diamonds). Also shown are radar lines from the IceBridge radar by Lewis et al. (2017) as well as

30   additional radar lines as presented in Karlsson et al. (2016) and Karlsson et al. (2020), the latter following along the same route as in this study from NEEM to EGRIP in 2015.
The average accumulation from both firn and snow core study sites are within uncertainties and in line with previous estimates. A particularly strong comparison is observed with the radar lines by Karlsson et al. (2020) representing the period 1694-2015 and the snow cores estimates by Schaller et al. (2016), representing 2014-2015. However, the mean annual accumulation

35   reconstructed as part of this study is more often than not increased compared to other previous estimates as evident in Figure 1 (especially east of the divide).
We observe no significant common trend in accumulation over time for the six firn cores and we find no evidence for the speculated accumulation change as a function of climate change for any of the six sites in the cores themselves. Whilst the trends are susceptible to the period investigated (10, 20, 30, and 40 yr periods), we do observe a decreasing trend for the period

40   2000-2010. This is equal to -1.40 cm w.eq. yr^{-2} in A1 in the west and -0.12 cm w.eq. yr^{-2} at site A4 in the east, although only significant within 95% at sites A1, A2 and A3.

The accumulation averages west of the divide (A1, A2) are in line with previous firn and radar estimates. Here we observe a period of increasing accumulation in the period 1988-1998 in the western cores (A1, A2 and A3), followed by a decrease towards 2015 for cores A1 and A2, a trend also observed in the HIRHAM5 model. In the firn cores A1 and A2 the years around 2000 show up as extreme accumulation years and enhances the trend.

5 Closer to the central ice divide the trends with time in cores A3 and A6 are insignificant, however we notice that the period 1995-2004 is high compared to other periods (Table 2). The firn accumulation reconstructions at these more central sites fall within previous estimates, whilst the model underestimates the accumulation.

East of the divide the extreme events seem more scattered and may be a result of local topography effects in combination with
10 depositional noise amplified at low accumulation sites. We observe a clear decrease in accumulation when moving east off the ice divide from the snow cores and an additional decrease when simultaneously moving northward. An increase compared to previous estimates is observed in the area around EastGRIP, but the site (A4 and A5) is highly influenced by the local topography of the north-east Greenland ice stream and additional spatial data are needed to constrain accumulation properly in this area.

15 Below the annual mean accumulation and their trends for each region is further discussed in detail.

4.3.1 North Greenland accumulation – West of the divide

The annual accumulation for the cores west of the divide (A1, A2 and A3) are highly correlated (>0.54, Table 4), a trend which is also observed in the HIRHAM5 model (>0.83). The accumulation means are close to previous firn and radar estimates, with a slight recent increase in accumulation at the NEEM site. We find in all three cores; A1, A2 and A3 that 1988-1998 is a period
20 of increasing accumulation followed by a decrease towards 2015. High precipitation is observed in 2000, 2001, and 2010.

Close to the NEEM deep ice core drilling site we retrieved the firn core T2015-A1 (Figure 2, blue line) with a mean accumulation of 22.2 cm w.eq. yr^{-1}, matching with the HIRHAM5 (6% difference on the mean). One could speculate that the NEEM ice core drilling camp structures and especially the dome in the period 2008 to 2015 have had an influence on the
25 accumulation and satellite observations. This theory is supported by stake measurements taken around NEEM which suggest an increase of accumulation around camp. We deliberately avoided such camp infrastructure interferences and drilled the core 5 km upwind from the main NEEM ice core camp location in the clean snow zone. Furthermore, we do not observe an increase nor decrease in accumulation compared to the remainder of the T2015-A1 record while NEEM was an active camp (2008-2012), but note that the years 2009, 2010 and 2011 are higher than surrounding years.

30 The NEEM deep ice core project lasted for several years and in the process several shallow firn and snow cores were retrieved. An average annual mean accumulation of 20.3±3.1 cm w.eq yr^{-1} over the past 3000 years is observed in the main NEEM ice core (Rasmussen et al., 2013) and a reconstruction using four firn cores retrieved close by covering the period 1727-2007 finds similar results (Masson-Delmotte et al., 2015). Our results are thus in the higher end of the previous ice core estimates. The radar lines from the traverse 2015 (Karlsson et al., 2020) show a similar mean to those from this study of 22.2 cm w.eq. yr^{-1}
35 for the period 1694-2015 and when compared with other nearby radar lines (Karlsson et al., 2016, 2020; Lewis et al., 2017), we find accumulation rates in close proximity to the NEEM drilling site that are also in line with our findings. This is particularly true when compared with the nearest Icebridge radar line, which shows for the period common with the T2015-A1 core an accumulation of 23.6±1.97 cm w.eq yr^{-1} and the snow core retrieved at NEEM during the N2E traverse, which has 22.7 cm w.eq yr^{-1} accumulation annually (Schaller et al., 2016). The more recent high estimates point to the period 1998-2015
40 as one high in accumulation compared to the past 300 years as observed by Masson-Delmotte et al. (2015), yet not as compared to the results from radar lines (Karlsson et al., 2020). However, Masson-Delmotte et al. (2015) did observe an increase in accumulation of 1.6 cm yr^{-1} per decade from 1980 to 2007. Such increasing trend is also supported by IceBridge radar and

HIRHAM5 modelling for the same period. But, our firn core T2015-A1 does not cover all of that particular period. Conversely, in the overlapping period from 1998-2015, we observe a decreasing trend in the accumulation of the core T2015-A1 with a total of -3.7 mm w.eq. yr^{-2}, a value highly influenced by the extreme years in 2000 and 2001. That trend is also found in both operation IceBridge retrieved radar data (-2,8 mm w.eq. yr^{-2}) and in the HIRHAM5 model (-1.3 mm w.eq. yr^{-2}). In addition,

5 we observe that 2009/2010 is extreme in accumulation in both model and reconstructed accumulation from the firn core at site A1.

In conclusion, at the NEEM site we find that the period 1998-2015 experienced increased accumulation compared to the previous ice core estimates by 9%, but not compared to radar and that throughout the periods 1998-2015 a decreasing trend was observed, mainly driven by extreme accumulation in 2000 and 2001 and that extreme accumulation was also found in

10 2010 in both firn and model.

At site T2015-A2 (Figure 2, red line) 100 km upstream from NEEM on the north western ice divide we reconstruct a mean accumulation of 17.6 cm w.eq. yr^{-1}, less than that found at the NEEM site. It however shares the same features of decreasing accumulation as observed near NEEM (core A2 -8.2 mm w.eq. yr^{-2}, IceBridge radar -9.3 mm w.eq. yr^{-2}). In addition the core

15 shows an increasing trend for the period 1988-1998 of 11 mm w.eq. yr^{-2}, a value also reflected to smaller extent in the HIRHAM model (+5.3 mm w.eq. yr^{-2}) and in the radar (+4.1 mm w.eq. yr^{-2}). The three closest snow cores obtained by Schaller et al., 2016 show an accumulation of 20.5, 17.2 and 19.3 cm w.eq. yr^{-1} and thus within the range observed in the firn core A2. Whilst the estimates from the IceBridge radar (19.09 cm w.eq yr^{-1}) are slightly larger, the model estimates a comparable value of 17.9 cm w.eq. yr^{-1} over the full length of the core (1988-2015). The B26 firn core from the NGT traverse retrieved in 1995 in

20 between our A1 and A2 sites, show for the period 1512-1994 an accumulation in line with the model and our results with a value of 17.9 cm w.eq. yr^{-1}. Thus our recent accumulation reconstruction point towards a steady accumulation, with the caveat that the position of the NGT core and our N2E core are 37 km apart. We do not observe any sign of the extreme accumulation in 2010 in A2 despite the HIRHAM5 model results.

25 Site T2015-A3 (Figure 2, green line) covers the same temporal period as A2 and also shows an increase in the period 1988-1998 (+8.8 mm w.eq yr^{-2}). However, unlike A1 and A2, no significant trend for the period following 1998 is observed. The site is an additional 94 km upstream from site T2015-A2 and is in general slightly lower in accumulation (17.5 cm w.eq. yr^{-1}). However, it is worth noting that at site A3 in general the HIRHAM5 model produces estimates of ~3 cm w.eq lower than those observed in the firn core, a constant offset that likely is a result of the ice divide position as discussed earlier. The IceBridge

30 radar trend over time does not match those trends observed in the firn core, however mean values are comparable with one another and also with the 2015 radar mean (Karlsson et al., 2020). The closest N2E snow core (Schaller et al., 2016) point towards slightly lower accumulation, and is in line with the model despite only covering only few years. During the 1994 NGT traverse, between A2 and A3 a core was collected (B27/28) and they observe 18.0 cm w.eq. annually for the period 1783-1993 (Weissbach et al., 2016). Given their similarity to the firn core results, this suggests no recent accumulation increase has been

35 observed at the T2015-A3 site.

4.3.2 North Greenland accumulation- at the central divide

In the dry central-Northern region we retrieved core T2015-A6 (Figure 2, yellow line) with 11.8 cm w.eq. yr^{-1}. At this low accumulation site the model underestimates the accumulation observed in the firn core by on average 2.5 cm w.eq. yr^{-1}. The closest IceBridge radar lines fit well in mean accumulation yet display slightly higher accumulation compared to the firn core

40 estimate for the period 1996-2014 and slightly lower accumulation than observed in the A6 core reconstruction from the 70's to the late 90's. The snow cores collected nearby also during the N2E traverse, which show accumulations of 11.7 and 12.7 cm w.eq. yr^{-1} (Schaller et al., 2016), are in line with our results as is the radar 2015 results (Karlsson et al., 2020). There are

no NGT traverse cores nearby, however A6 is positioned almost half way between NGT core B18 and B29 (Figure 1). These earlier cores have annual accumulations of 10.3 and 14.9 cm w.eq. yr^{-1} respectively and align well with our results. At A6 we observe a small decreasing trend since the mid 1990's (-2.4 mm w.eq. yr^{-2}), which is stronger when focusing on the past 10 years (-6.3 mm w.eq. yr^{-2}). Such a trend is not captured in the model nor in the radar.

4.3.3 Northern accumulation east of the main ice divide (snow cores 2017).

Further south we observe a decreasing trend in accumulation when moving north and eastward from the central divide as a result of the divide shielding from the western precipitation as evidenced from the snow cores retrieved from the Inuit Windsled Project traverse in 2017. The snow cores cover a line of 280 km, ~265 km in a north-south direction and ~100 km in the east–west direction with an altitude decrease of 150 m when moving north-east (Figure 1, Table 5). The accumulation in 2015-2016 summer is spanning 24.5 cm to 15.4 cm w.eq. yr^{-1}.

The closest older points of observation are the NGT snow cores (Burkhart et al., 2009) and the radar line (Karlsson et al., 2020) all of which are east of our snow cores (Figure 1). The NGT results and radar lines support an eastern decreasing precipitation trend for this area of the Greenland ice sheet. Furthest south and 100 km east of the core-WP 726 (24.5 cm w.eq), a NGT core is found with 15.5 cm w.eq annually (Burkhart et al., 2009). Half way on the transect and about 80 km east of the snow core WS 2017-5 (18.6 cm w.eq), the longer NGT firn core B16 displays a mean accumulation of 14.1 cm w.eq annually for the period 1640-1993 (Weissbach et al., 2016). Lastly, in the north 40 km east of the sites WS2017-6 (16.1 cm w.eq. yr^{-1}) and WP 606 (15.4 cm w.eq. yr^{-1}), NGT snow core has a value of 13.3 cm w.eq. yr^{-1} (Burkhart et al., 2009), supporting the decrease trend in accumulation when moving both east and north. We restrain from speculating on any accumulation trend over time for this area as the NGT snow cores, radar line and our snow cores are far apart and because our cores represent just one year of accumulation.

4.3.4 EastGRIP accumulation

Close to the EastGRIP ice core drilling site and only 15 km apart from the location where both the core T2015-A4 and T2015-A5 were drilled, an annual accumulation 14.1 and 14.7 cm w.eq. yr^{-1} was observed for the period 1997-2015. Similar observations were also produced by the three closest snow cores taken during the 2015 traverse with values of 13.2 14.6 and 14.0 cm w.eq. yr^{-1} (Schaller et al., 2016). Similar results were also present within traverse radar lines (13.0 w.eq. yr^{-1} (Karlsson et al., 2020)) and from two 4 metre snowpits, where accumulations of 13.8 and 14.5 cm w.eq. yr^{-1} where observed (Nakazawa et al., 2020). These values are all larger than the older estimate of 11.6 cm w.eq. yr^{-1} from the North East Greenland Ice Stream within the similar period (NEGIS, (Vallelonga et al., 2014)) and also larger than the NGT traverse snow cores taken in the area in the early 90's (11.6 and 12.9 cm w.eq. yr^{-1}). The discrepancy to recent firn and snow results could be interpreted as a recent increase in accumulation compared to the 1990's (NGT cores). However we note that when comparing the overlapping time period with of our firn core (1966-2012) that NEGIS results also show a lower 11.2+-1.6 cm w.eq. yr^{-1} than the A5 core having 13.8 cm w.eq. yr^{-1} (Table 3). Furthermore, the trend observed in our A4 and A5 core shows increased accumulation in the 1990's compared to the mean and thus a discrepancy between our results and those from the NEGIS firn core exist in this area.

In addition we observe that the accumulation in A4 and A5 firn cores are poorly correlated (R^2 -0.28) and that the trend in both cores is variable. The reconstructed accumulation from A4 and A5 are poorly correlated also with the HIRHAM5 model accumulation. However, in the model domain the correlation between the sites just 10's of km apart is excellent (0.97). We explain the discrepancies with the position of the cores close to the North East Greenland Ice Stream. The North East Greenland Ice Stream (NEGIS) is the largest ice stream in Greenland and the central velocity close to EGRIP is larger than 60 m yr^{-1} in the area. The strain from the ice stream compared to the surrounding stagnant ice forms local topographic hills both with

minima on the shear margin and as undulating waves along the ice stream itself (Fahnestock et al., 2001; Joughin et al., 2010; Vallelonga et al., 2014).

Figure 6 shows the area close to EGRIP, the location of A4 and A5 and the ice sheet surface altitude. The NEGIS core is at the centre of the ice stream (close to deep ice core EastGRIP being drilled these years), while core A4 is outside the main ice

5 stream on the shear margin and A5 is outside the shear margin to the north in "stagnant" ice. All three NGT firn cores (Weissbach et al., 2016) are similar to A4 on the shear margin to the northern side of the ice stream. Further upstream compared to A4 and the snow core WP506 retrieved in 2017 is even further upstream, but again on the shear margin. Thus we hypothesize that the variability between A4 and the older snow cores from the NGT traverse is caused by local topography influencing the shear margin and thus the local accumulation.

10 Site A5 is in the stagnant ice outside the ice stream and shows a more regular deposition from the mid 80's, except for the extreme 2010 year. Prior to the mid 80's the core has increased variability compared to the latter period. This is contrary to the model and ice bridge radar, which show increasing accumulation (1 and 3 mm w.eq. yr^{-1} respectively) from the mid 80's. Both in the core and in the radar a higher accumulation is observed in the late 60's. However, we note that the uncertainty associated with the timescales of cores A4 and A5 allow for changes that could influence the trends discussed, especially in

15 the deeper part of the cores.

In conclusion the accumulation reconstructed from firn and snow cores around EastGRIP seem to be influenced by local topographic variations caused by the North East Greenland Ice Stream. As such any accumulation record from this site should be carefully analysed in relation to the local constraints. To truly resolve this areas accumulation structure and any temporal

20 trend and to determine how the EastGRIP deep ice core can be analysed as a proxy of past climate, a fine grid of cores or radar analysis for reconstructing accumulation will be necessary.

5 Conclusion

In this study we have increased the number of recent accumulation constraints in central northern Greenland by adding six shallow firn cores and eight snow cores. We find no joined trend in the northern accumulation, thought to be a result of the

25 inter-annual noise in the reconstructions. In general our findings point to slightly larger accumulation in the northern Greenland area than that mapped by Burgess et al. (2010), especially around EastGRIP in the Northeast. The results are generally in line with previous ice cores and radar estimates, especially for the most recent two decades. The comparison to the P-E from the HIRHAM model show that the model tends to underestimate the accumulation compared to our findings from the firn core in the central north and east of the divide, a relevant finding for people reconstructing the surface mass balance.

30 The three traverse cores taken west of the divide tell a similar story of increasing accumulation in the 90's with a subsequent decrease from the millennia onwards. This trend is also supported by radar and reanalysis data though the trends in these are less. All three sites west of the divide are well correlated (>0.54) and a decrease in accumulation from the NEEM site (T2015-A1) is observed with a value of 22.2 cm w.eq yr^{-1} moving up the ice divide to site T2015-A3 (17.5 cm w.eq yr^{-1}). In general, the mean accumulation from the 3 western cores show similar accumulation to previous estimates. We find increased

35 temperatures of ~3°C since 1993 based on borehole temperature evidence. However, when looking into the details of the temperature versus the accumulation a Clausius-Clapeyron relationship trend is not observed on neither an annual basis nor in the mean trend in our reconstructed accumulation, despite a clear relation between temperature and precipitation in the re-analysis (R^2>0.6). In addition, we find some evidence of 2000's extreme accumulation in the firn cores A1 and A2.

When moving from the centre of Greenland north-east off the divide in the northern central Greenland we observe a decrease

40 in accumulation as also reconstructed from snow cores retrieved in 2017. Comparison with the older NGT snow cores

(Weissbach et al., 2016) and the radar line (Karlsson et al., 2020) further supports such a spatial variability. The HIRHAM5 models capture less of the observed accumulation when moving eastwards off the divide.

Close to EastGRIP the firn cores A4 and A5 are influenced by local topographic variations caused by the north east Greenland Ice Stream. Whilst A4 and A5 match well with previous accumulation estimates from snow pits (Nakazawa et al., 2020;

5 Schaller et al., 2016) the previous results from the NEGIS ice core do not (Vallelonga et al., 2014). We advise that any accumulation record from this site should be carefully analysed in relation to the local constrains. To truly resolve this area's accumulation structure additional firn reconstructions are necessary and a fine grid of cores upstream will be crucial to better understand the topographic influence on the EastGRIP deep ice core, if climate is to be reconstructed from it. At the EastGRIP site in the model the relationship between accumulation and temperature is less evident than to the west (R<0.3).

10 In conclusion, despite our findings of a significant north Greenland ice sheet warming of 0.9 to 2.5C/decade no common northern increasing trend in accumulation was observed in the firn cores as a result thereof. The overall spatial pattern of accumulation resembles previous estimates with the exception of sites close to the NEGIS ice stream, where we find larger accumulations than previous reported. The spatial variability observed in P-E from re-analysis data matches well, but our estimates of accumulation from the firn and snow cores were in general larger than the HIRHAM5 model estimates, except

15 close to the NEEM ice core drilling site. This general higher accumulation should be accounted for when modelling the current state of the Greenland ice sheet.

Data availability

The firn core T2015-A1 to T 2015-A6 and snow core from 2017 accumulation reconstructions will be made available at
20 relevant depositories upon publication.

Author contribution

HK and PV collected the samples during the field season 2015 joined by SK, NK and DDJ. RE collected snow cores during the Inuit Windsled Project traverse 2017 and JB was part of expedition organizing via the Dark Snow Project. HK, PZ, PV,
25 KHL, AS, SB measured the firn cores by means of CFA. PV, HAK, RE measured the wind sledge snow cores by means of CFA. MS and DDJ measured the water isotopes in firn cores A1 and A5. BV and CTH analysed the water isotopes and deuterium excess. HK and PZ made the annual layer counting and reconstructed the accumulation and further analysed the accumulation and chemistry data. MO and RM provided the re-analysis data and the HIRHAM modelling. GL provided nearest neighbour IceBridge radar data and NK radar from the traverse 2015. All authors contributed to the writing of the paper.

30

Acknowledgements

The research leading to these results has received funding from the European Research Council under the European Community's Seventh Framework Programme (FP7/2007-2013) / ERC grant agreement 610055 as part of the ice2ice project.

This project has received funding from the European Union's Horizon 2020 research and innovation programme under grant
35 agreement No 820970 as part of the TiPES project and is TiPES paper #50.

We acknowledge EGRIP and NEEM ice core drilling projects. EGRIP is directed and organized by the Center of Ice and Climate at the Niels Bohr Institute. It is supported by funding agencies and institutions in Denmark (A. P. Møller Foundation, University of Copenhagen), USA (US National Science Foundation, Office of Polar Programs), Germany (Alfred Wegener Institute, Helmholtz Centre for Polar and Marine Research), Japan (National Institute of Polar Research and Arctic Challenge
40 for Sustainability), Norway (University of Bergen and Bergen Research Foundation), Switzerland (Swiss National Science

Foundation), France (French Polar Institute Paul-Emile Victor, Institute for Geosciences and Environmental research) and China (Chinese Academy of Sciences and Beijing Normal University). NEEM is directed and organized by the Center of Ice and Climate at the Niels Bohr Institute and US NSF, Office of Polar Programs. It is supported by funding agencies and institutions in Belgium (FNRS-CFB and FWO), Canada (NRCan/GSC), China (CAS), Denmark (FIST), France

5 (IPEV, CNRS/INSU, CEA and ANR), Germany (AWI), Iceland (RannIs), Japan (NIPR), Korea (KOPRI), The Netherlands (NWO/ALW), Sweden (VR), Switzerland (SNF), United Kingdom (NERC) and the USA (US NSF, Office of Polar Programs). Sepp Kipfstuhl have received support from the Villum Investigator Project IceFlow (no. 16572).

We would also like to acknowledge financial support of the Dark Snow Project and the Inuit Windsled Project and within it especially Hermenegildo Moreno, Jens Jacob Simonsen and Ramon Larramendi.

References

Bales, R. C., Guo, Q., Shen, D., McConnell, J. R., Du, G., Burkhart, J. F., Spikes, V. B., Hanna, E. and Cappelen, J.: Annual
15 accumulation for Greenland updated using ice core data developed during 2000–2006 and analysis of daily coastal meteorological data, J. Geophys. Res. Atmospheres, 114(D6), doi:10.1029/2008JD011208, 2009.

Bamber, J. L., Layberry, R. L. and Gogineni, S. P.: A new ice thickness and bed data set for the Greenland ice sheet: 1. Measurement, data reduction, and errors, J. Geophys. Res. Atmospheres, 33773–33780, doi:10.1029/2001JD900054@10.1002/(ISSN)2169-8996.PARCA1, 2018.

20 Bigler, M., Svensson, A., Kettner, E., Vallelonga, P., Nielsen, M. E. and Steffensen, J. P.: Optimization of High-Resolution Continuous Flow Analysis for Transient Climate Signals in Ice Cores, Environ. Sci. Technol., 45(10), 4483–4489, doi:10.1021/es200118j, 2011.

Box, J. E.: Greenland Ice Sheet Mass Balance Reconstruction. Part II: Surface Mass Balance (1840–2010), J. Clim., 26(18), 6974–6989, doi:10.1175/JCLI-D-12-00518.1, 2013.

25 Box, J. E., Yang, L., Bromwich, D. H. and Bai, L.-S.: Greenland Ice Sheet Surface Air Temperature Variability: 1840–2007, J. Clim., 22(14), 4029–4049, doi:10.1175/2009JCLI2816.1, 2009.

Buchardt, S. L., Clausen, H. B., Vinther, B. M. and Dahl-Jensen, D.: Investigating the past and recent δ¹⁸O-accumulation relationship seen in Greenland ice cores, Clim. Past, 8(6), 2053–2059, doi:10.5194/cp-8-2053-2012, 2012.

30 Burgess, E. W., Forster, R. R., Box, J. E., Mosley-Thompson, E., Bromwich, D. H., Bales, R. C. and Smith, L. C.: A spatially calibrated model of annual accumulation rate on the Greenland Ice Sheet (1958–2007), J. Geophys. Res. Earth Surf., 115(F2), doi:10.1029/2009JF001293, 2010.

Burkhart, J. F., Bales, R. C., McConnell, J. R., Hutterli, M. A. and Frey, M. M.: Geographic variability of nitrate deposition and preservation over the Greenland Ice Sheet, J. Geophys. Res. Atmospheres, 114(D6), doi:10.1029/2008JD010600, 2009.

35 Christensen, O. B., Drews, M., Christensen, J. H., Dethloff, K., Ketelsen, K., Hebestadt, I. and Rinke, A.: The HIRHAM regional climate model version 5., DMI Technical Report, DMI, Copenhagen, Denmark. [online] Available from: https://www.dmi.dk/fileadmin/Rapporter/TR/tr06-17.pdf, 2006.

Clow, G. D.: The extent of temporal smearing in surface-temperature histories derived from borehole temperature measurements, Palaeogeogr. Palaeoclimatol. Palaeoecol., 98(2), 81–86, doi:10.1016/0031-0182(92)90189-C, 1992.

40 Dahl-Jensen, D., Mosegaard, K., Gundestrup, N., Clow, G. D., Johnsen, S. J., Hansen, A. W. and Balling, N.: Past Temperatures Directly from the Greenland Ice Sheet, Science, 282(5387), 268–271, doi:10.1126/science.282.5387.268, 1998.

Dee, D. P., Uppala, S. M., Simmons, A. J., Berrisford, P., Poli, P., Kobayashi, S., Andrae, U., Balmaseda, M. A., Balsamo, G., Bauer, P., Bechtold, P., Beljaars, A. C. M., van de Berg, L., Bidlot, J., Bormann, N., Delsol, C., Dragani, R., Fuentes, M., Geer, A. J., Haimberger, L., Healy, S. B., Hersbach, H., Hólm, E. V., Isaksen, L., Kållberg, P., Köhler, M., Matricardi, M.,

McNally, A. P., Monge-Sanz, B. M., Morcrette, J.-J., Park, B.-K., Peubey, C., de Rosnay, P., Tavolato, C., Thépaut, J.-N. and Vitart, F.: The ERA-Interim reanalysis: configuration and performance of the data assimilation system, Q. J. R. Meteorol. Soc., 137(656), 553–597, doi:10.1002/qj.828, 2011.

Eerola, K: About the performance of HIRLAM version 7.0, HIRLAM Newsl., 51, 93–102, 2006.

5 Fahnestock, M., Abdalati, W., Joughin, I., Brozena, J. and Gogineni, P.: High geothermal heat flow, Basal melt, and the origin of rapid ice flow in central Greenland, Science, 294(5550), 2338–2342, doi:10.1126/science.1065370, 2001.

Fischer, H., Wagenbach, D. and Kipfstuhl, J.: Sulfate and nitrate firn concentrations on the Greenland ice sheet: 2. Temporal anthropogenic deposition changes, J. Geophys. Res. Atmospheres, 103(D17), 21935–21942, doi:10.1029/98JD01886, 1998.

Frey, M. M., Bales, R. C. and McConnell, J. R.: Climate sensitivity of the century-scale hydrogen peroxide (H2O2) record
10 preserved in 23 ice cores from West Antarctica, J. Geophys. Res. Atmospheres, 111(D21), doi:10.1029/2005JD006816, 2006.

Gfeller, G., Fischer, H., Bigler, M., Schüpbach, S., Leuenberger, D. and Mini, O.: Representativeness and seasonality of major ion records derived from NEEM firn cores, The Cryosphere, 8(5), 1855–1870, doi:https://doi.org/10.5194/tc-8-1855-2014, 2014.

Gkinis, V., Popp, T. J., Blunier, T., Bigler, M., Schüpbach, S., Kettner, E. and Johnsen, S. J.: Water isotopic ratios from a
15 continuously melted ice core sample, Atmospheric Meas. Tech., 4(11), 2531–2542, doi:10.5194/amt-4-2531-2011, 2011.

Gundestrup N. S., Clausen H. B. and Hansen B. L.: The UCPH borehole logger, , 49, 224–233, 1994.

Hanna, E., Cappelen, J., Fettweis, X., Mernild, S. H., Mote, T. L., Mottram, R., Steffen, K., Ballinger, T. J. and Hall, R. J.: Greenland surface air temperature changes from 1981 to 2019 and implications for ice-sheet melt and mass-balance change, Int. J. Climatol., n/a(n/a), doi:10.1002/joc.6771, n.d.

20 Hawley, R. L., Courville, Z. R., Kehrl, L. M., Lutz, E. R., Osterberg, E. C., Overly, T. B. and Wong, G. J.: Recent accumulation variability in northwest Greenland from ground-penetrating radar and shallow cores along the Greenland Inland Traverse, J. Glaciol., 60(220), 375–382, doi:10.3189/2014JoG13J141, 2014.

Hutterli, M. A., Raible, C. C. and Stocker, T. F.: Reconstructing climate variability from Greenland ice sheet accumulation: An ERA40 study, Geophys. Res. Lett., 32(23), doi:10.1029/2005GL024745, 2005.

25 Jansen, E., Christensen, J. H., Dokken, T., Nisancioglu, K. H., Vinther, B. M., Capron, E., Guo, C., Jensen, M. F., Langen, P. L., Pedersen, R. A., Yang, S., Bentsen, M., Kjær, H. A., Sadatzki, H., Sessford, E. and Stendel, M.: Past perspectives on the present era of abrupt Arctic climate change, Nat. Clim. Change, 10(8), 714–721, doi:10.1038/s41558-020-0860-7, 2020.

Johnsen, S. J., Dansgaard, W. and White, J. W. C.: The origin of Arctic precipitation under present and glacial conditions, Tellus B Chem. Phys. Meteorol., 41(4), 452–468, doi:10.3402/tellusb.v41i4.15100, 1989.

30 Johnsen, S. J., Clausen, H. B., Dansgaard, W., Gundestrup, N., Hansson, M., Johnsson, P., Steffensen, J. P. and Sveinbjørnsdottir, A. E.: A "deep" ice core from East Greenland, Meddelelser Om Grønl. Geosci., 29, 1992.

Johnsen, S. J., Clausen, H. B., Cuffey, K. M., Hoffmann, G., Schwander, J. and Creyts, T.: Diffusion of stable isotopes in polar firn and ice : the isotope effect in firn diffusion, Phys. Ice Core Rec., 121–140, 2000.

Joughin, I., Smith, B. E., Howat, I. M., Scambos, T. and Moon, T.: Greenland flow variability from ice-sheet-wide velocity
35 mapping, J. Glaciol., 56(197), 415–430, doi:10.3189/002214310792447734, 2010.

Karlsson, N. B., Eisen, O., Dahl-Jensen, D., Freitag, J., Kipfstuhl, S., Lewis, C., Nielsen, L. T., Paden, J. D., Winter, A. and Wilhelms, F.: Accumulation Rates during 1311–2011 CE in North-Central Greenland Derived from Air-Borne Radar Data, Front. Earth Sci., 4, doi:10.3389/feart.2016.00097, 2016.

Karlsson, N. B., Razik, S., Hörhold, M., Winter, A., Steinhage, D., Binder, T. and Eisen, O.: Surface accumulation in Northern
40 Central Greenland during the last 300 years, Ann. Glaciol., 61(81), 214–224, doi:10.1017/aog.2020.30, 2020.

Kaufmann, P. R., Federer, U., Hutterli, M. A., Bigler, M., Schüpbach, S., Ruth, U., Schmitt, J. and Stocker, T. F.: An Improved Continuous Flow Analysis System for High-Resolution Field Measurements on Ice Cores, Environ. Sci. Technol., 42(21), 8044–8050, doi:10.1021/es8007722, 2008.

Nakazawa, F., Nagatsuka, N., Hirabayashi, M., Goto-Azuma, K., Steffensen, J. P. and Dahl-Jensen, D.: Variation in recent annual snow deposition and seasonality of snow chemistry at the east Greenland ice core project (EGRIP) camp, Greenland, Polar Sci., 100597, doi:10.1016/j.polar.2020.100597, 2020.

Orsi, A. J., Cornuelle, B. D. and Severinghaus, J. P.: Little Ice Age cold interval in West Antarctica: Evidence from borehole 5 temperature at the West Antarctic Ice Sheet (WAIS) Divide, Geophys. Res. Lett., 39(9), doi:10.1029/2012GL051260, 2012.

Orsi, A. J., Kawamura, K., Masson-Delmotte, V., Fettweis, X., Box, J. E., Dahl-Jensen, D., Clow, G. D., Landais, A. and Severinghaus, J. P.: The recent warming trend in North Greenland, Geophys. Res. Lett., 44(12), 6235–6243, doi:10.1002/2016GL072212@10.1002/(ISSN)2169-9291.ARCTICJOINT, 2017.

Rasmussen, S. O., Abbott, P. M., Blunier, T., Bourne, A. J., Brook, E., Buchardt, S. L., Buizert, C., Chappellaz, J., Clausen, 10 H. B., Cook, E., Dahl-Jensen, D., Davies, S. M., Guillevic, M., Kipfstuhl, S., Laepple, T., Seierstad, I. K., Severinghaus, J. P., Steffensen, J. P., Stowasser, C., Svensson, A., Vallelonga, P., Vinther, B. M., Wilhelms, F. and Winstrup, M.: A first chronology for the North Greenland Eemian Ice Drilling (NEEM) ice core, Clim. Past, 9(6), 2713–2730, doi:10.5194/cp-9-2713-2013, 2013.

Roeckner, E., Bäuml, G., Bonaventura, L., Brokopf, R., Esch, M., Giorgetta, M., Hagemann, S., Kirchner, I., Kornblueh, L. 15 and Manzini, E.: The atmospheric general circulation model ECHAM 5. PART I: Model description, 2003.

Röthlisberger, R., Bigler, M., Hutterli, M., Sommer, S., Stauffer, B., Junghans, H. G. and Wagenbach, D.: Technique for Continuous High-Resolution Analysis of Trace Substances in Firn and Ice Cores, Environ. Sci. Technol., 34(2), 338–342, doi:10.1021/es9907055, 2000.

Sandberg Sørensen, L., Simonsen, S. B., Forsberg, R., Khvorostovsky, K., Meister, R. and Engdahl, M. E.: 25 years of 20 elevation changes of the Greenland Ice Sheet from ERS, Envisat, and CryoSat-2 radar altimetry, Earth Planet. Sci. Lett., 495, 234–241, doi:10.1016/j.epsl.2018.05.015, 2018.

Schaller, C. F., Freitag, J., Kipfstuhl, S., Laepple, T., Steen-Larsen, H. C. and Eisen, O.: A representative density profile of the North Greenland snowpack, The Cryosphere, 10(5), 1991–2002, doi:https://doi.org/10.5194/tc-10-1991-2016, 2016.

Sigg, A. and Neftel, A.: Seasonal Variations in Hydrogen Peroxide in Polar Ice Cores, Ann. Glaciol., 10, 157–162, 25 doi:10.3189/S0260305500004353, 1988.

Simonsen, M. F., Cremonesi, L., Baccolo, G., Bosch, S., Delmonte, B., Erhardt, T., Kjær, H. A., Potenza, M., Svensson, A. and Vallelonga, P.: Particle shape accounts for instrumental discrepancy in ice core dust size distributions, Clim. Past, 14(5), 601–608, doi:https://doi.org/10.5194/cp-14-601-2018, 2018.

Simonsen, S. B. and Sørensen, L. S.: Implications of changing scattering properties on Greenland ice sheet volume change 30 from Cryosat-2 altimetry, Remote Sens. Environ., 190, 207–216, doi:10.1016/j.rse.2016.12.012, 2017.

Steen-Larsen, H. C., Masson-Delmotte, V., Sjolte, J., Johnsen, S. J., Vinther, B. M., Bréon, F.-M., Clausen, H. B., Dahl-Jensen, D., Falourd, S., Fettweis, X., Gallée, H., Jouzel, J., Kageyama, M., Lerche, H., Minster, B., Picard, G., Punge, H. J., Risi, C., Salas, D., Schwander, J., Steffen, K., Sveinbjörnsdóttir, A. E., Svensson, A. and White, J.: Understanding the climatic signal in the water stable isotope records from the NEEM shallow firn/ice cores in northwest Greenland, J. Geophys. Res. 35 Atmospheres, 116(D6), doi:10.1029/2010JD014311, 2011.

Steffen, K. and Box, J.: Surface climatology of the Greenland Ice Sheet: Greenland Climate Network 1995–1999, J. Geophys. Res. Atmospheres, 33951–33964, doi:10.1029/2001JD900161@10.1002/(ISSN)2169-8996.PARCA1, 2018.

Svensson, A., Andersen, K. K., Bigler, M., Clausen, H. B., Dahl-Jensen, D., Davies, S. M., Johnsen, S. J., Muscheler, R., Parrenin, F., Rasmussen, S. O., Röthlisberger, R., Seierstad, I., Steffensen, J. P. and Vinther, B. M.: A 60 000 year Greenland 40 stratigraphic ice core chronology, Clim. Past, 4(1), 47–57, 2008.

Vallelonga, P., Christianson, K., Alley, R. B., Anandakrishnan, S., Christian, J. E. M., Dahl-Jensen, D., Gkinis, V., Holme, C., Jacobel, R. W., Karlsson, N. B., Keisling, B. A., Kipfstuhl, S., Kjær, H. A., Kristensen, M. E. L., Muto, A., Peters, L. E., Popp, T., Riverman, K. L., Svensson, A. M., Tibuleac, C., Vinther, B. M., Weng, Y. and Winstrup, M.: Initial results from geophysical surveys and shallow coring of the Northeast Greenland Ice Stream (NEGIS), Cryosphere, 8(4), 1275–1287, 45 doi:10.5194/tc-8-1275-2014, 2014.

Weissbach, S., Wegner, A., Opel, T., Oerter, H., Vinther, B. M. and Kipfstuhl, S.: Spatial and temporal oxygen isotope variability in northern Greenland – implications for a new climate record over the past millennium, Clim. Past, 12, 171–188, doi:Weissbach, S. , Wegner, A. , Opel, T. ORCID: https://orcid.org/0000-0003-1315-8256 <https://orcid.org/0000-0003-1315-8256>, Oerter, H. , Vinther, B. M. and Kipfstuhl, S. (2016) Spatial and temporal oxygen isotope variability in northern

Greenland – implications for a new climate record over the past millennium , Climate of the Past, 12 , pp. 171-188 . doi:https://doi.org/10.5194/cp-12-171-2016 <https://doi.org/10.5194/cp-12-171-2016> , hdl:10013/epic.46817, 2016.

Winstrup, M., Svensson, A. M., Rasmussen, S. O., Winther, O., Steig, E. J. and Axelrod, A. E.: An automated approach for annual layer counting in ice cores, Clim. Past Discuss., 8(6), 1881–1895, doi:10.5194/cp-8-1881-2012, 2012.

Table 1. Name, Latitude, Longitude, Altitude and lengths of the shallow firn cores and snow cores presented in this study. The firn cores are labelled 2015T-A1 (NEEM ice core drilling site) to 2015T-A5 (EastGRIP drilling site). All cores were drilled in 2015 and measured by means of CFA in Copenhagen in 2017/2018.

Firn core		Coordinates		Altitude	Depth of core	Time period covered
ID		N	W	m a.s.l.	m	AD
2015 (NEEM)	T-A1	77N25.219'	51W09.588'	2484	9.08	2015-1998 (±1)
2015 T-A2		77N01.764'	47W28.832'	2620	10.74	2015-1988 (±1)
2015 T-A3		76N27.290'	44W47.709'	2771	10.97	2015-1988 (±0)
2015 T-A4		75N41.340'	36W28.926'	2701	10.91	2015-1982 (±2)
2015 (EGRIP)	T-A5	75N37.501'	35W58.809'	2708	14.02	2015-1966 (±2)
2015 T-A6		76N10.294'	41W05.628'	2760	12.07	2015-1968 (±3)

Table 2. Temperatures. Site ID, 10 m depth temperature in the borehole at site, Water isotope derived temperature using the relationship T = (δ18O+13.7)/0.67, HIRHAM annual mean temperature, HIRHAM temperature in 2014, HIRHAM temperature in 1993, 15 m depth temperatures determined in close by boreholes during the North Greenland Traverse 1993-1995, closest B core to
10 **the here presented firn cores are chosen for comparison. Ordered by the shallow firn cores used in this study 2015T-A1 (NEEM ice core drilling site) to 2015T-A5 (EastGRIP drilling site).**

Firn core	Temperature ~10 m within snowpack 2015	Temperature ~mean over full firn core from water isotopes	Temperature ~Annual mean 1980 to 2014 from HIRHAM	Temperature ~Annual mean 2014 from HIRHAM	Temperature ~Annual mean 1993 from HIRHAM	Temperature ~15 m within snowpack from closest NGT core 1993-1995
ID	°C	°C (‰)	°C	°C	°C	°C
2015 T-A1 (NEEM)	-27.4 (-9.0 m)	-27.6 (32.17)	-24.51	-21.96	-24.42	-30.3 (B26)
2015 T-A2	-26.7 (-10.7 m)		-25.88	-22.36	-25.83	-30.6 (B27/28)
2015 T-A3	-29.8 (-10.9 m)		-26.97	-24.47	-27.06	
2015 T-A4	-28.8 (-10.0 m)		-27.30	-24.31	-27.52	
2015 T-A5 (EGRIP)	-29.2 (-10.0 m)	-33.5 (36.15)	-27.14	-24.15	-27.32	-32.3 (B17)
2015 T-A6	-29.0 (-10.1 m)		-27.55	-24.76	-27.97	

Table 3: Decadal water equivalent annual accumulation as observed from the firn cores 2015TA1 to 2015T-A6. The cores are ordered with A1 being most west and the last (A5) most eastward (ordering is also north to south). Also shown is the mean for the overlapping periods between the cores (1997-2014) and the full core accumulation mean.

Core	1965-1974 [m w.eq. a^{-1}]	1975-1984 [m w.eq. a^{-1}]	1985-1994 [m w.eq. a^{-1}]	1995-2004 [m w.eq. a^{-1}]	2005-2014 [m w.eq. a^{-1}]	1997-2014 [m w.eq. a^{-1}]	Full core [m w.eq. a^{-1}]
A1	-	-	-	*0.255 ± 0.038**	0.215 ± 0.040	0.235 ± 0.041*	0.222 ± 0.056
A2	-	-	*0.164 ± 0.052***	0.227 ± 0.029	0.146 ± 0.021	0.183 ± 0.049	0.176 ± 0.050
A3	-	-	*0.153 ± 0.023***	0.195 ± 0.017	0.180 ± 0.010	0.186 ± 0.016	0.175 ± 0.028
A6	*0.103 ± 0.011*****	0.122 ± 0.018	0.123 ± 0.012	0.133 ± 0.015	0.112 ± 0.025	0.121 ± 0.024	0.118 ± 0.022
A4	-	*0.179 ± 0.007****	0.147 ± 0.044	0.152 ± 0.024	0.143 ± 0.019	0.141 ± 0.023	0.146 ± 0.031
A5	*0.136 ± 0.056******	0.111 ± 0.044	0.152 ± 0.020	0.143 ± 0.026	0.153 ± 0.047	0.147 ± 0.039	0.137 ± 0.042

* Only years 1998-2004; ** Only years 1988-1994; *** Only years 1982-1984

5   **** only years 1966-1974 *****1968-1974

10   **Table 4: Annual mean accumulation pearson correlations (R^2) between sites as observed in the firn core for their overlapping period; 1998-2015 and in the HIRHAM5 model domain. Model correlations are in italic. Correlations are shown in bold if p<0.02.**

Core / Core	A1	A2	A3	A4	A5	A6
A1	1	**0.56**/*0.89*	**0.79**/*0.83*	0.37/*0.13*	0.51/*0.20*	**0.73**/*0.29*
A2		1	**0.54**/*0.95*	0.38/*0.38*	0.32/*0.44*	**0.55**/*0.55*
A3			1	**0.54**/*0.43*	0.33/*0.49*	**0.62**/*0.64*
A4				1	0.28/***0.97***	0.18/***0.74***
A5					1	0.36/***0.76***
A6						1

Table 5: Accumulation from the snow cores collected during the 2017 wind sledge traverse from summer 2015-summer

15   **2016.**

Firn core	Coordinates		Depth of core	Time period covered	Accumulation 2015 summer- 2016 summer
ID	N	W	m	AD	[m w.eq.a^{-1}]
WP726	73°33.360'N	40°33'50.00''W	2	2017-2013	0.245
WS2017-5	73°55'40.344'N	40°09'09.00''W	2	2017-2012	0.186

WP 706	73°43'51.00"N	40°25'46.00"W	2	2017-2012	0.179
WP656	74° 08'46.08"N	39°52'1.74"W	2	2017-2012	0.161
WP2017-6	74° 20'21.00"N	39°25'31.00"W	2	2017-2012	0.161
WP 606	74°31'6.623"N	38°55'11.08"W	2	2017-2012	0.154
WS2017-7	74°42'59.50"N	38°31'20.80"W	2	2017-2012	0.151
WP 506	75°15'55.00"N	37°1'41.00"W	2	2017-2012	0.140
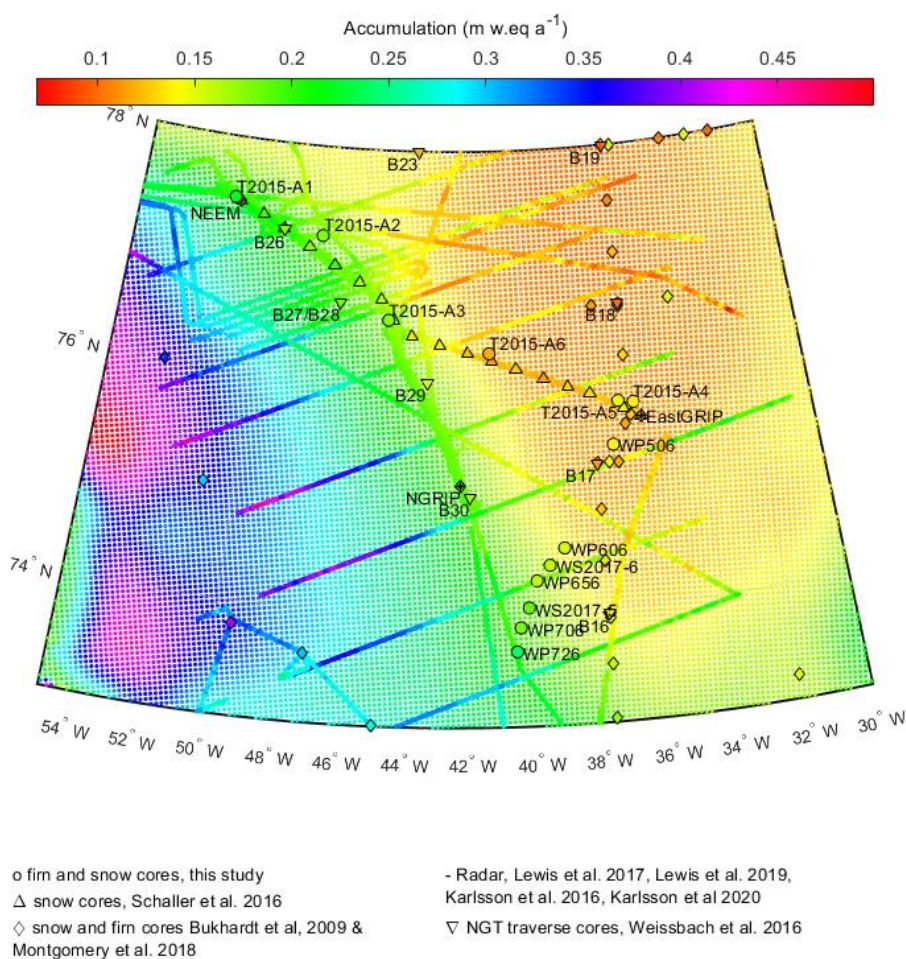
Figure 1: Map of North Greenland accumulation. Color scale indicate the accumulation in m w.eq. yr⁻¹ from Burgess et al., 2010.
Circles indicate the position of the 6 firn cores drilled in Northern Greenland (T2015-A1 to T2015-A6, table 1) and the 2017 snow
10 cores (WPxxx and WS2017-x, table 5) from this study. Note that the cores T2015-A1 (NEEM site) to T2015-A3 all are on the local
western ice divide. T2015-A6, is located on the central ice divide and T2015-A4 and T2015-A5 are on the east side of the divide
located close to the EastGRIP ice core drilling site (details shown in figure 6). The 2017 snow cores are all east of the divide. In
addition accumulation from snow cores collected in 2015 is shown (Schaller et al., 2016) **indicated by a triangle facing up,**

accumulation estimates from the deep Greenland ice cores (*), accumulation from the NGT traverse cores taken from the 1993-1995 (triangle facing down, (Weissbach et al., 2016)), data collected as part of the sum up dataset (Montgomery et al., 2018) including snow and ice cores as well as stake measurements (diamonds) as well as radar lines from Karlsson et al., 2016; Lewis et al., 2017, 2019; Karlsson et al., 2020.
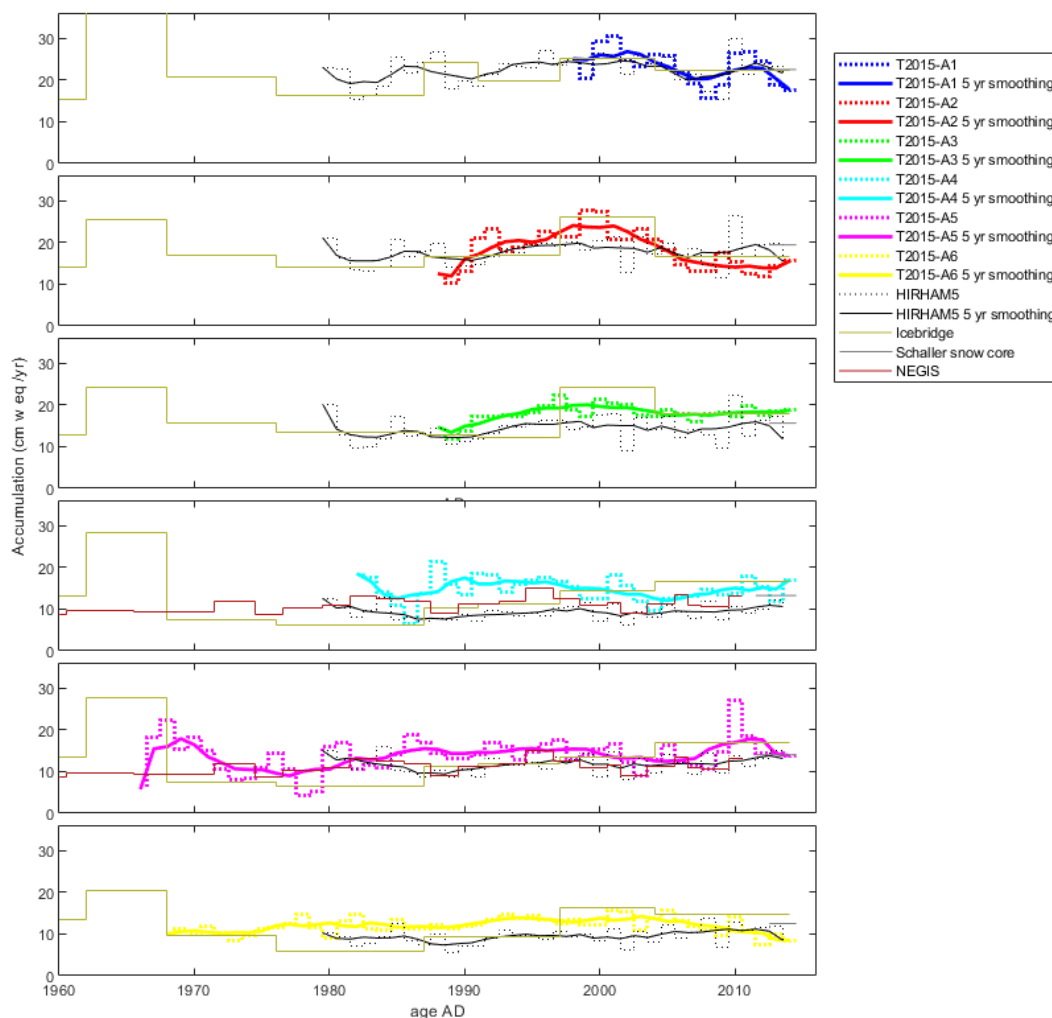
Figure 2: Accumulation with time. Dashed coloured lines show annually reconstructed accumulation from the firn cores in m w.eq. a^{-1}, while thick lines are the 5 yr running average; A1 (blue), A2 (red), A3 (green), A4 (cyan), A5 (purple) and A6 (yellow). In dashed black is shown the HIRHAM5 annual precipitation minus evaporation for the 6 sites and full black is the 5 year running average from the model. In brown is shown IceBridge radar results of the accumulation between dated horizons (Gabriel Lewis et al. 2017)

10   and in grey accumulation from snow cores take in 2015 as presented in Schaller et al., 2016. For the cores A4 and A5 the NEGIS ice core is also shown ((Vallelonga et al., 2014)).
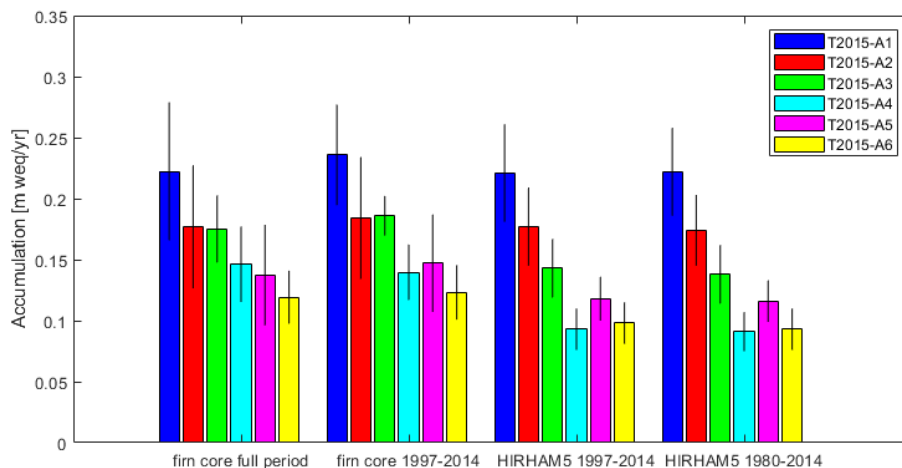
Figure 3: Mean accumulation from the firn cores (two sets of left most) and for the HIRHAM5 model for the closest model grid (two sets of right most). The period 1997-2014 is directly comparable (centre), for completion also the full firn records (most left) are shown and the full reconstruction period (right most) are shown. For the cores A1 (blue), A2 (red), A3 (green), A4 (cyan), A5 (purple) and A6 (yellow).
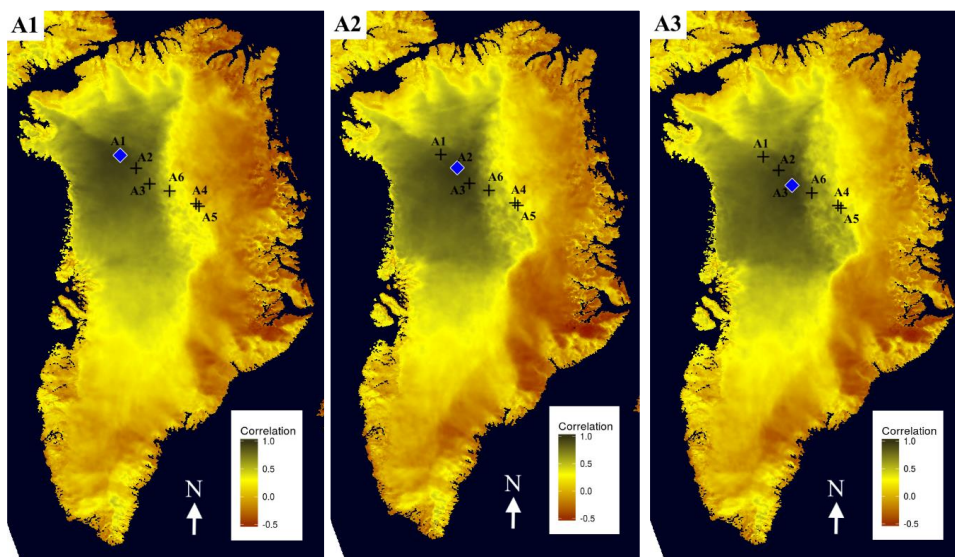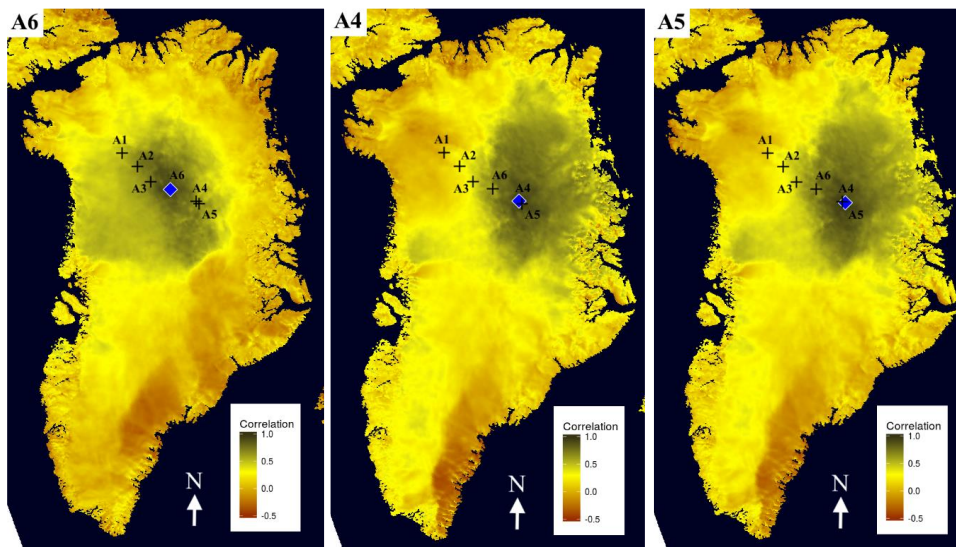
Figure 4: Correlation maps of Greenland from HIRHAM5 reanalyses for the locations of the cores A1-A6, based on annual average precipitation minus evaporation records. Darker green area represents grid points that correlate well with R-values of up to 1, while lighter yellow areas show no correlation at all.
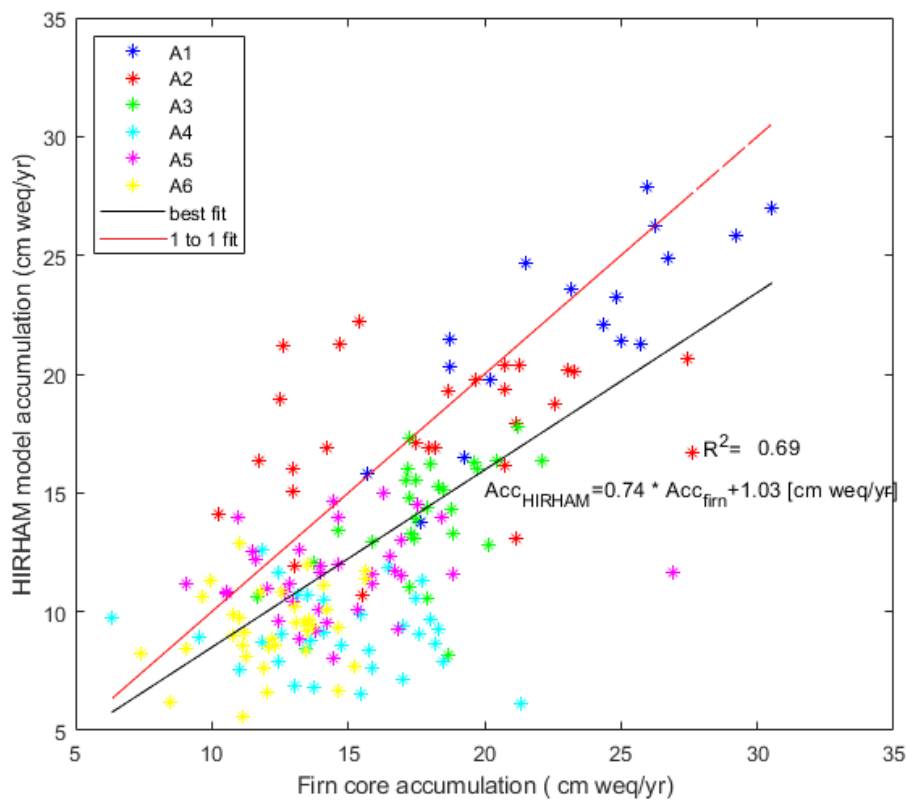
Figure 5: Annual mean accumulation from HIRHAM reanalyses plotted against the firn annual mean accumulation reconstructions for the cores A1-A6. Using data from all cores the correlation is 0.69 (CI 0.61, CI 0.76). The model consequently underestimates the accumulation we observe in the firn cores.
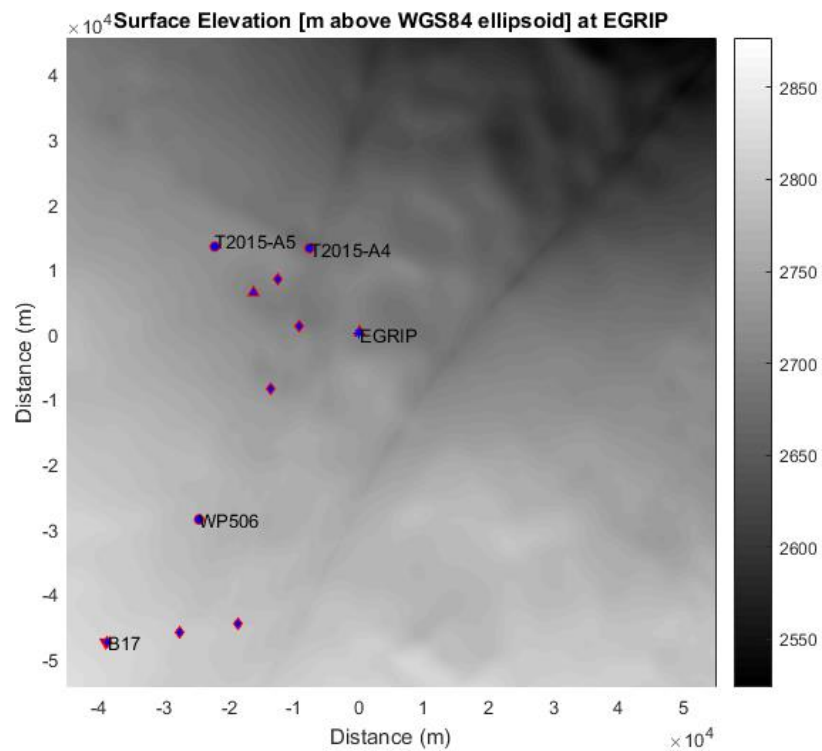
Figure 6: Surface elevation (m above the WGS84 ellipsoid of the local area close to the EastGRIP deep ice core drilling site shown
10 **together with the firn cores obtained in this study T2015 A4 and T 2015 A5 (circles), snow cores from the same traverse in 2015 (triangles), snow core from 2017 (WP506), as well as other snow and firn cores (diamonds).**
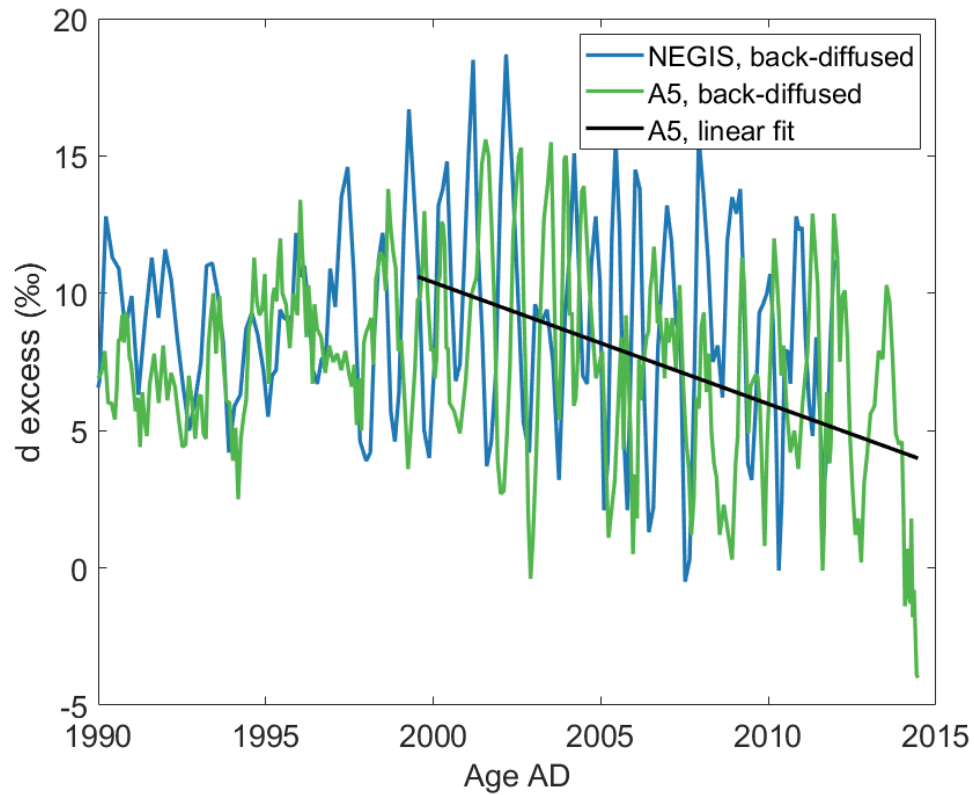
Figure 7: In green back-diffused d-excess from the A5 core, compared with previous determined d-excess from the NEGIS firn core (Vallelonga et al., 2014). As well as a linear fit for the A5 core over the period where the back-difussion can be trusted.